

# Principal Component Analysis to Identify Parameters in MRgFUS Treatment

LILLA BONANNO<sup>1</sup>, AUGUSTO IELO<sup>1</sup>, SERENA DATTOLA<sup>1</sup>, VALENTINA HARTWIG<sup>2</sup>,  
ROSA MORABITO<sup>1</sup>, SIMONA CAMMAROTO<sup>1</sup>, CHIARA SMORTO<sup>1</sup>, ANNALISA MILITI<sup>1</sup>,  
CARMELO ANFUSO<sup>1</sup>, GIUSEPPE DI LORENZO<sup>1</sup>, CHIARA SORBERA<sup>1</sup>, AMELIA BRIGANDI<sup>1</sup>,  
ANTONIO CERASA<sup>3,4,5</sup>, ALBERTO CACCIOLA<sup>6</sup>, SILVIA MARINO<sup>1</sup>, ANGELO QUARTARONE<sup>1</sup>,  
GIUSEPPE ACRI<sup>7</sup>

<sup>1</sup>IRCCS Centro Neurolesi Bonino Pulejo, Via Palermo Ctr. Casazza, 98123, Messina, ITALY

<sup>2</sup>Institute of Clinical Physiology (IFC), Italian National Research Council (CNR), 56124 Pisa, ITALY

<sup>3</sup>Institute for Biomedical Research and Innovation (IRIB),  
National Research Council of Italy (CNR), Messina, ITALY

<sup>4</sup>S. Anna Institute, Crotone, ITALY

<sup>5</sup>Pharmacotechnology Documentation and Transfer Unit,  
Preclinical and Translational Pharmacology, Department of Pharmacy,  
Health Science and Nutrition, University of Calabria, 87036 Arcavacata, ITALY

<sup>6</sup>Brain Mapping Lab, Department of Biomedical, Dental Sciences and  
Morphological and Functional Imaging, University of Messina, Messina, ITALY

<sup>7</sup>Department of Biomedical, Dental Sciences and Morphological and Functional Imaging,  
University of Messina, Messina, ITALY

**Abstract:** - Magnetic Resonance-guided Focused Ultrasound Surgery (MRgFUS) is a relatively new treatment which combines the precision of radiological imaging with the therapeutic potential of focused ultrasound, promising a non-invasive treatment for different conditions. The objective of this work was to apply Principal Component Analysis (PCA) to identify the main factors that influence the efficacy of MRgFUS treatment. Thirty-six neurological patients with medication-refractory tremor (n=19 Parkinson's Disease (PD); n=17 Essential Tremor (ET)) were treated with a commercial MRgFUS brain system (ExAblate Neuro 4000, InSightec) integrated with a 1.5T Magnetic Resonance Imaging (MRI) unit (Sigma HDxt; GE Medical System). We applied PCA, using Kaiser's criterion, to guide principal component maintenance. The most significant variables for these components, based on the magnitude of their loadings, were maximum energy delivered (Joule) for PC1 (eigenvalues=3.85), indicating the influence of energy delivery; Cerebrospinal Fluid Volume (CSV) normalized for PC2 (eigenvalues=2.55), highlighting CSF; White Matter Volume (WMV) normalized for PC3 (eigenvalues=1.50), reflecting WMV; and active elements for PC4 (eigenvalues=1.18). Few studies have highlighted the influence of energy delivery on treatment outcomes, aligning with our results where maximum energy delivered (PC1) demonstrated a predominant impact. In conclusion, the application of PCA, as guided by Kaiser's rule, has not only facilitated a robust analysis of MRgFUS treatment variables but also set a benchmark for future research in this field. This study contributes to support the clinical value of PCA as a powerful analytical tool to personalize, precision-focused neurological treatment.

**Key-Words:** - Magnetic Resonance-guided Focused Ultrasound Surgery; Principal Component Analysis; Parkinson's Disease; Essential Tremor; Energy delivery; Cerebrospinal Fluid Volume normalized; White Matter Volume normalized; Active elements; Medical ultrasonics.

Received: March 3, 2024. Revised: August 3, 2024. Accepted: September 2, 2024. Available online: October 3, 2024.

## 1 Introduction

Principal Component Analysis (PCA) is a powerful and versatile statistical technique that simplifies complex data sets by reducing their dimensionality. This technique finds extensive use in various fields, including medical research, where it is crucial for the

analysis and interpretation of multidimensional data, [1]. PCA demonstrates to be particularly valuable as it reduces data dimensionality while preserving the most relevant information. This is essential in studies where parameters are numerous and potentially interrelated, as in the case of functional magnetic reso-

nance imaging (fMRI), Electroencephalography application (EEG), [2], and in Magnetic Resonance-guided Focused Ultrasound (MRgFUS), [3]. In the context of MRgFUS treatment, the importance of PCA becomes particularly evident. The effectiveness of this therapy could be different for numerous physiological and technical parameters, making it crucial to identify and understand the most significant factors influencing treatment outcomes.

Neurological disorders such as essential tremor (ET) and Parkinson's disease (PD) can be treated using various non-invasive methods besides MRgFUS, such as Transcranial Magnetic Stimulation (TMS), [4], Transcranial Direct Current Stimulation (tDCS), [5], and Low-Intensity Focused Ultrasound (LIFU), [6]. Comparatively, MRgFUS offers real-time monitoring and the ability to create precise, adjustable lesions without ionizing radiation. However, it faces challenges such as skull density limitations and the need for specialized equipment. Understanding the landscape of these non-invasive therapies is crucial for the development and refinement of MRgFUS techniques, [3]. [7], conducted a pivotal study demonstrating the clinical benefits of MRgFUS thalamotomy for ET, reporting significant improvements in tremor scores and patient quality of life. The study reported in [8], examined the cognitive, mood, and quality-of-life outcomes after MRgFUS thalamotomy, providing a comprehensive assessment of the broader impacts of the treatment beyond motor symptom relief. The MRgFUS treatment induces an immediate clinical reduction of symptoms by inflicting a thermal lesion on the ventral intermediate (VIM) thalamic nucleus. Generally, 3-months after intervention, the beneficial clinical effects persisted in most patients with a mean improvement in hand tremor score of 47%, compared to 0.1% in the sham surgery group at the same time point, [9]. Intraoperative MR imaging is critical for accurately targeting anatomical structures, as well as for designing and tracking the necessary number of sonications to accomplish therapeutic ablation, [10]. Moreover, to ensure sustained clinical benefits, it is essential to create a lesion of the correct size, [11]. The quantity of acoustic energy needed to generate a lesion in the brain through MRgFUS is different for patients. This variance is due to the acoustic characteristics and the density of brain tissues (such as White Matter (WM), Grey Matter (GM), and Cerebrospinal Fluid (CSF)) which affect how much energy is transmitted as opposed to reflected or absorbed, [12], [13], [14]. The skull bone primarily obstructs the passage of ultrasound waves into the brain. Before initiating treatment, the skull density ratio (SDR) is typically calculated to evaluate the skull's ultrasound transparency, [15]. High SDR values ( $SDR > 0.45$ ) correlate positively with the max-

imal temperature achieved ( $T_{max}$ ), while low SDR values ( $SDR < 0.40$ ) present technical challenges, such as prolonged treatment duration or the need for increased energy, [16]. Recent findings by [17], indicate that MRgFUS treatment for ET is more effective with an SDR of at least 0.45, though it can still be conducted efficiently and safely with an SDR as low as 0.3. Contrarily, research by [18], showed that there was no significant statistical difference in the mean SDR among patients who experienced lasting symptoms improvement and those who saw symptoms recurrence, even in trials including patients with an SDR below 0.40. The rate at which temperature rises during thermal ablation is a critical factor for the success of the procedure. Typically, achieving accurate necrosis requires at least two sonications at a temperature of  $56^{\circ}\text{C}$ , [8]. Therefore, identifying the factors contributing to temperature increases is crucial for improving the efficacy of these treatments, [19]. In terms of predicting lesion size following repeated sonications, both the Accumulated Thermal Dose (ATD) and the mean  $T_{max}$  achieved have proven to be useful indicators. [20], found that ATD values could predict the size of lesions in ET patients one day after MRgFUS treatment. Nonetheless, ATD does not appear to correlate with SDR values, [8], while [21], established a correlation between SDR and both the Joules and maximum temperatures reached within the lesion. The complex relationship between patient-specific biological traits (such as age, brain volumes, skull density, cortical thickness) and parameters related to MRgFUS treatment (such as SDR, ATD, and mean  $T_{max}$ ) determine the success of thermal lesion formation. The application of PCA allows to extract the principal components that influence treatment efficacy, thereby facilitating an understanding of the complex dynamics involved and guiding the development of more effective and personalized therapeutic protocols, [22], [23]. Through understanding these key parameters can improve the development of targeted, effective and individualized treatment protocols. The application of PCA should allow more accurate hypotheses to be made about how MRgFUS works and improve patient selection criteria, thereby increasing the likelihood of treatment success. This approach aims to uncover the complex interactions that influence treatment efficacy and refine treatment strategies accordingly. MRgFUS presents a sophisticated therapeutic option, but its success is influenced by multiple complex factors. Identifying these factors is crucial for optimizing treatment outcomes. Previous research has primarily focused on individual parameters without fully integrating them into a comprehensive analysis. In our study, the aim was to use PCA to identify the main factors that influence the efficacy of MRgFUS treatment, to fill that

gap by using PCA to identify the most influential parameters, providing a comprehensive understanding of the factors affecting MRgFUS efficacy.

## 2 Methods

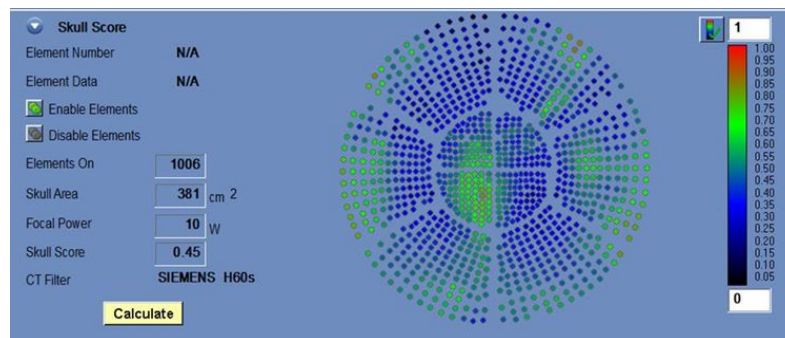
All procedures were approved by the internal Ethics Committee of the IRCCS Bonino-Pulejo, the MRgFUS VIM thalamotomy screening and surgery (CE n.38/2021). All participants provided written informed consent before their clinical data was used in the study. Patients suffering from medication-resistant tremor-dominant neurological disorders, notably PD and ET, were treated at IRCCS Bonino-Pulejo, Messina, Italy, using the MRgFUS brain system from April 19, 2019, to December 31, 2021. These patients exhibited clinically significant tremors that did not respond to dopaminergic or anticholinergic medications. Specifically, Essential Tremor patients had to demonstrate intact nigrostriatal dopaminergic terminals, confirmed by a normal dopamine transporter scan (DaT-SCAN). Patients were excluded if they had cognitive decline as assessed by the Core Assessment Program for Surgical Interventional Therapies in Parkinson's Disease (CAPSIT-PD), [24], unstable or severe psychiatric conditions such as anxiety or depression, a history of substance abuse as per the DSM-5 criteria, or a history of epileptic seizures. The radiological criteria for MRgFUS eligibility included the absence of intracranial hemorrhage, ischemic stroke, neoplasms, intracranial aneurysms, or arteriovenous malformations requiring treatment, and a SDR greater than 0.35 based on screening Computed Tomography (CT) scans. Clinical criteria excluded patients on unintermittent anticoagulant therapy, and those with significant unstable medical conditions. Thirty-six patients with hemidominant tremor met these criteria and were subsequently treated with MRgFUS (19 with PD and 17 with ET). PD patients with an average age of  $69.1 \pm 7.6$  years and a mean disease duration of  $8.8 \pm 5.1$  years; ET patients with an average age of  $67.7 \pm 10.1$  years and a mean disease duration of  $18.7 \pm 15.5$  years. All PD patients were evaluated using the Movement Disorder Society Unified Parkinson's Disease Rating Scale motor section under (MDS-UPDRS-III) defined OFF-medication (at least 12 hours after discontinuing any anti-parkinsonian medication) and ON-medication (90 minutes after a levodopa loading dose roughly equal to 150% of the patient's usual morning dose of dopaminergic medication) conditions. Medication-resistant tremor was defined as patients who showed no significant improvement in tremor subscales between ON- and OFF-medication states.

### 2.1 Acquisition CT and MRI'Ucanning in MRgFUS Treatment Planning

All participants underwent pre-operative instrumental evaluations, including brain CT and Magnetic Resonance Imaging (MRI) scans, and clinical assessments. Screening CT images were obtained using a 64-slice multidetector CT scanner (SOMATOM Definition AS, Siemens Healthineers, Erlangen, Germany). The imaging protocol consisted of sequential acquisition without gantry tilt; a tube voltage of 120 kV and a tube current of 220 mA; a slice thickness of 0.6 mm, with no spacing between slices; and images were reconstructed using the B60f sharp – Osteo setting. The SDR was calculated on the MRgFUS workstation (Neuroablate 4000, Insightech, Israel) by aligning MRI and CT head images. Patients underwent a comprehensive neuroimaging evaluation using a 3T whole-body MRI scanner (Achieva, Philips Medical System, Best, the Netherlands) before their treatment. This scanner was equipped with a 32-element phased array sensitivity-encoding (SENSE) head coil and featured gradients capable of a maximum slew rate of 200 mT/m/ms and a maximum gradient strength of 80 mT/m. The imaging protocol comprised 3D T1-weighted Magnetization Prepared Rapid Gradient Echo (MP-RAGE), 3D Fluid-Attenuated Inversion Recovery (3D-FLAIR), two-dimensional coronal and axial T2-weighted Fast Spin Echo (FSE), and axial Susceptibility Weighted Imaging (SWI). For the 3D T1-weighted MP-RAGE, parameters included a Repetition Time (TR) of 8.2 ms, an Echo Time (TE) of 3.7 ms, a section thickness of 1 mm, averaging one signal, and a reconstruction matrix of 512x512. The 3D-FLAIR images were captured with a TR of 12000 ms, a TE of 140 ms, an Inversion Time (TI) of 285 ms, a section thickness of 4 mm, averaging one signal, and a reconstruction matrix of 512x512. T2-weighted FSE images featured a TR of 4100 ms, a TE of 100 ms, a section thickness of 2-3 mm, averaging one signal, and a reconstruction matrix of 512x512. SWI images were acquired with a TR of 31 ms, a TE of 7.2 ms, a section thickness of 3 mm, and a reconstruction matrix of 512x512. These MR images played a pivotal role in prospective pre-operative planning.

### 2.2 MRgFUS Treatment: Techniques and Protocols

The MRgFUS thalamotomies were conducted using the ExAblate Neuro 4000, a focused ultrasound (FUS) system from InSightec, Haifa, Israel, coupled with a 1.5T MRI unit (Sigma HDxt; GE Medical System). One of the advantages of MRgFUS is its ability to modulate brain functions without causing physical lesions. Unlike deep brain stimulation, which re-



"Fig01: Visualization of Skull Score Distribution and MRgFUS Treatment Parameters. The left side lists the key procedural parameters, including the number of active elements, skull area, focal power, skull score, and the type of CT filter used. The right side features a skull score map, color-coded to show the varying transmission characteristics across the skull surface

quires the use of depth electrodes and pulse generators, MRgFUS operates through low-frequency sonication. This approach not only avoids the need for invasive approach but also allows for safe subsequent treatments if needed. Studies have demonstrated the efficacy of FUS in blocking nerve conduction, which could be beneficial for treating neurological conditions characterized by dysfunctional networks, [25], [26]. Moreover, low-frequency MRgFUS is being explored in both human and animal studies for its potential to enhance the delivery of chemotherapy, stem cells, or gene therapies to specific brain areas by temporarily disrupting the blood-brain barrier using microbubble expansion, [27]. Initially, the patient's scalp was shaved and a stereotactic frame was applied under local anesthesia. A flexible silicone membrane was then placed on the patient's head before they were positioned on the MRI table. Attached to the membrane, a 30-cm diameter hemispheric, 1024-element, phased-array ultrasound transducer operating at 650kHz facilitated the treatment. To prevent thermal damage to the skin and skull, degassed cooled water circulated within the membrane between the head and the transducer. Before of procedure, a 2 mm thick 3D fast-recovery fast spin echo (FRFSE) T2-weighted image was acquired to determine stereotactic coordinates and plan the target area. Treatment planning involved aligning CT and MRI scans, marking calcifications and frontal sinuses as "no pass" regions, and calculating the number of transducer elements required to deliver the necessary energy. Fiducial markers were also placed on live MR images to track any movement automatically. As the VIM nucleus is not visible via standard MRI sequences, its location was determined using distance measurements from known anatomical landmarks. The target position was set based on intraoperative T2-weighted images at 14-15 mm lateral from the midline, 10-11 mm lateral from the third ventricle's wall, one quarter of

the total AC-PC line distance anterior of the PC, and 1.5-2 mm above the AC-PC plane.

### 2.3 Setting Parameters in MRgFUS Treatment

In the MRgFUS procedure, precise alignment of the treatment target is a critical initial step to ensure the effectiveness of the focused ultrasound. This alignment is confirmed through two short (10-second) and low-power (250W) sonications that increase temperatures between 40°C and 45°C. The use of MR thermometry during these preliminary sonications allows for precise alignment of the focal heating volume by monitoring the proton resonance frequency (PRF) shift in water molecules. The MR thermometry sequence parameters are carefully set (TR/TE 26.172 ms/12.996 ms, slice thickness 3 mm, FOV 28x28 cm², matrix size 256x128, and a temporal resolution of 3.5 ms) to provide accurate intraoperative temperature calculations, which are crucial for achieving correct targeting before proceeding with higher-intensity sonications. The initial low-power sonications serve multiple purposes of minimize the risk of unintended tissue damage while confirming the accuracy of the targeting. By observing the temperature response, clinicians can ensure that the focal point of the ultrasound beam is correctly aligned with the intended target area, thereby reducing the risk of off-target effects during the subsequent higher-power sonications. Once the correct alignment is confirmed, the procedure advances by increasing the power of the high-intensity focused ultrasound (HI-FU) beam to achieve temperatures within the 50°C-54°C range. This intermediate temperature range is chosen to induce a transient clinical effect, allowing for real-time assessment of the treatment's impact on the patient's symptoms, such as tremor suppression. Subsequently, sonication power and/or duration are gradually increased to reach therapeutic temperature levels (55°-60°C). This

gradual escalation is critical because it allows the formation of the lesion to be carefully monitored and controlled, reducing the likelihood of excessive heating that could damage surrounding tissues. Adjustments are made based on real-time clinical feedback, including the degree of tremor suppression and any side effects observed, ensuring that the treatment is both effective and safe. Post-procedure, Fast Recovery Fast Spin Echo (FRFSE) T2-weighted images are obtained on the axial plane to visualize the resulting thalamic lesion. These images provide critical confirmation of the lesion's size and location, ensuring that the treatment has been applied correctly. Comprehensive documentation of the treatment includes key technical parameters, such as:

- *Number of Active Elements*: The count of active transducer elements used during sonication, which influences the precision and intensity of the energy delivered (Fig. 1).
- *Skull Surface Area*: A factor that affects how the ultrasound energy is transmitted through the skull, influencing the effectiveness of the treatment (Fig. 1).
- *Maximum Energy Delivered (Joules)*: The total energy applied during the treatment, which is crucial for achieving the desired therapeutic effect.
- *Maximum Power (Watts) and Sonication Time (Seconds)*: These parameters determine the intensity and duration of each sonication, which must be carefully balanced to achieve sufficient heating without causing collateral damage.
- *Maximal Temperature (°C)*: The peak temperature achieved during treatment, which directly impacts the extent of tissue ablation.
- *Area Temperature Dose (ATD)*: Calculated from the thermometric map of the final sonication, the ATD provides a measure of the thermal dose received by the target area, with the region of interest (ROI) manually defined at the target.

The specific settings chosen for each parameter are based on their proven ability to optimize the balance between efficacy and safety. Energy and Power Settings are adjusted to ensure sufficient energy delivery to induce the necessary thermal effect while minimizing the risk of overheating. The gradual increase in sonication duration and temperature is tailored to the patient's response, allowing for personalized treatment that maximizes clinical benefits and minimizes risks. Continuous monitoring using MR thermometry ensures precise control over the treatment process,

enabling real-time adjustments and enhancing overall treatment safety.

## 2.4 Methodological Approach for the Extraction of Parameters from Structural MRI

Before undergoing MRgFUS treatment, a detailed examination of the brain tissue—comprising white matter (WM), gray matter (GM), and cerebrospinal fluid (CSF)—is conducted to assess the volume between the target area and the transducers. The analysis of structural imaging data was performed using SPM12 ([www.fil.ion.ucl.ac.uk](http://www.fil.ion.ucl.ac.uk)), while the CAT12 toolbox (<http://www.neuro.uni-jena.de/cat/>, version r1109) within the MATLAB environment ([www.mathworks.com](http://www.mathworks.com), Version 2015a) was used to perform the volumetric analysis. Images of each participant were reoriented to align with the anterior commissure as the origin point and standardized for spatial orientation. A non-linear deformation field was then calculated to optimally match the tissue probability maps to the individual scans. The gray matter volume (GMV) and total intracranial volume (TIV) were calculated, focusing specifically on GM tissue. Subsequently, all tissue segments in native space were aligned to the MNI (Montreal Neurological Institute) standard template included in SPM12 using an affine registration algorithm. The DARTEL (Diffeomorphic Anatomical Registration Through Exponentiated Lie Algebra) toolbox further refined the inter-subject registration of GM and WM. In DARTEL's final step, GM tissues were modulated using a non-linear deformation method to allow comparison of relative GMV, adjusted for individual brain sizes. Additionally, the voxel values in the tissue maps were adjusted based on the Jacobian determinant calculated during spatial normalization, [28]. A quality check using the CAT12 toolbox assessed the homogeneity of the GM tissues post-processing. Each participant's modulated and normalized GM tissue segments were then smoothed with an 8-mm full width at half maximum Gaussian filter. Total cortical thickness for all individuals was also estimated using the CAT12 toolbox within SPM12, leveraging MATLAB (version 2015a). The initial ROI analysis segmented volumes based on surface and thickness estimates, employing the projection-based thickness (PBT) method to simultaneously estimate central surface and cortical thickness, [29]. This step included topology correction, spherical mapping, and registration, with local maximum in the GM projected to neighboring voxels based on WM distance post-segmentation, [30]. Additionally, the extent of white matter T2 hyperintense lesions, typically indicative of chronic small vessel ischemia, was quantified by us-

ing the Fazekas scale, [31].

### 3 Data Analysis Methods Description

The PCA method transforms a set of correlated variables into a new set of independent variables known as principal components. The variables involved in the analysis of dependent components are derived from both MRgFUS parameters (SDR, Skull area, Active elements, Number of sonications, maximum watt, maximum joule, mean maximal temperature, maximum sonication Time, ATD) and volumetric measures (Fazekas, Normalized GMV, Normalized WMV, Normalized CSFV, Normalized TIV, Thickness). Analyses were performed using the open source R4.2.2 software package (R Foundation for Statistical Computer, Vienna, Austria). An initial cleaning such as the removal of unnecessary columns and standardization was performed. Standardization, a critical step in PCA, ensures that all variables are on an equal footing by having a mean of zero and a variance of one. This eliminates the bias due to different scales of measurement in the original variables. The standardization formula for each variable is given by equation 1:

$$z_{ij} = \frac{x_{ij} - \bar{x}_j}{s_j} \quad (1)$$

where  $z_{ij}$  is the standardized value for the  $i$ -th observation of the  $j$ -th variable,  $x_{ij}$  is the original value of the  $i$ -th observation of the  $j$ -th variable,  $\bar{x}_j$  is the mean of the  $j$ -th variable and  $s_j$  is the standard deviation of the  $j$ -th variable.

After standardization, the covariance matrix  $C$  of the standardized variables is calculated. This matrix computes both the principal components and their associated standard deviations, which are then squared to obtain the eigenvalues. The formula for the covariance matrix is given by equation 2:

$$C = \frac{1}{n-1} Z^T Z \quad (2)$$

where  $C$  represents the covariance matrix,  $Z$  contains the standardized data,  $Z^T$  is the transpose of the matrix  $Z$ ,  $n$  is the number of observations, and  $n-1$  in the denominator corrects for the bias in the estimation.

The eigenvalues and eigenvectors of the covariance matrix  $C$  are calculated to identify the principal components. We applied Kaiser's Rule, which recommends retaining only those components with an eigenvalue greater than 1, in order to determine the number of significant components.

The eigenvalues  $\lambda_i$  and eigenvectors  $v_i$  are the solutions to the characteristic equation 3:

$$Cv_i = \lambda_i v_i \quad (3)$$

Eigenvalues indicate the amount of variance explained by each principal component, while eigenvectors define the direction of these components in the original space of the variables. Principal components are calculated as linear combinations of the original variables, weighted according to the eigenvectors. The  $k$ -th principal component,  $PC_k$  given by equation 4:

$$PC_k = Zv_k \quad (4)$$

where  $PC_k$  represents the  $k$ -th principal component,  $Z$  is the matrix of standardized data,  $v_k$  denotes the  $k$ -th eigenvector. The percentage of variance explained by each principal component is calculated using the eigenvalues. The variance explained by the  $k$ -th component given by equation 5:

$$Explained\ Variance_k = \frac{\lambda_k}{\sum_{i=1}^p \lambda_i} \quad (5)$$

where  $Explained\ Variance_k$  is the proportion of the total variance that is explained by the  $k$ -th principal component, where  $\lambda_k$  is the eigenvalue associated with the  $k$ -th principal component and  $p$  is the total number of components. Furthermore, the cumulative explained variance is useful for determining the number of components to retain. It is calculated by progressively summing the variance explained by each component 6:

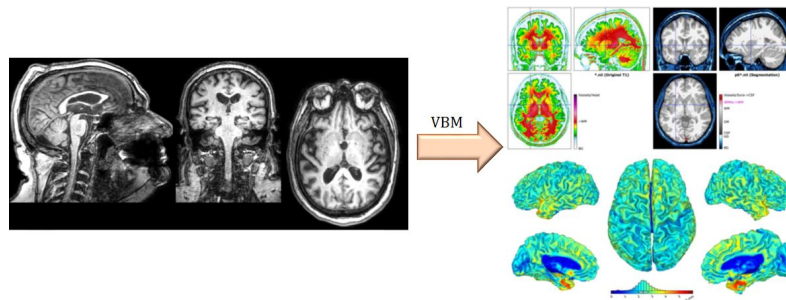
$$Cumulative\ Explained\ Variance_k = \sum_{i=1}^k Explained\ Variance_i \quad (6)$$

where  $Cumulative\ Explained\ Variance_k$  is the total variance explained by the first  $k$  components, summing the explained variances from the 1st to the  $k$ -th component.

### 4 Results

Thirty-six neurological patients with hemi-dominant tremor satisfied the clinical criteria and were assigned to MRgFUS treatment (19 PD and 17 ET). A pre-treatment MRI exam was employed for brain volumetric quantification. Table 1 presents the mean values and standard deviations of MRI parameters for patients, which include measurements such as Normalized Gray Matter Volume (GMV), White Matter Volume (WMV), and Cerebrospinal Fluid (CSF) volumes, as well as Total Cortical Thickness and the





"Fig02: Workflow and Results of Voxel-Based Morphometry (VBM) Analysis. The left side displays the original MRI scans in sagittal, coronal, and axial views, highlighting the brain's anatomy. The right side presents the processed VBM results, including heatmaps of tissue volumes and 3D reconstructions of cortical grey matter distribution. This figure demonstrates how VBM analysis enhances the understanding of brain structure by quantifying and visualizing tissue volume variations across different regions

Fazekas Scale score (Fig. 2). The overall MRI-based averages and standard deviations of the procedural parameters employed during VIM thalamotomy in the neurological patients are shown in Table 2. These detailed parameters provide insights into the physiological and procedural aspects influencing the effectiveness and safety of MRgFUS treatments in neurological patients. The enrolled patients had side effects over the course of the treatment. Before PCA, two essential statistical tests were conducted: the Kaiser-Meyer-Olkin (KMO) measure of sampling adequacy and Bartlett's test of sphericity. The KMO measure evaluates how well the data is suited for PCA. A KMO value closer to 1 indicates that the data is highly suitable for PCA, as the variables share a common variance, making them appropriate for structure detection. Bartlett's test assesses whether the correlation matrix of the data is an identity matrix, which would suggest that the variables are unrelated and unsuitable for PCA. A significant result ( $p$ -value  $< 0.05$ ) implies that the data's correlations are sufficient to warrant the use of PCA. The KMO value obtained was 0.82, which indicates that the data is highly suited for PCA. This value surpasses the commonly accepted threshold of 0.6, confirming the adequacy of the data for factor analysis. The test returned a chi-square value of 254.63 with a  $p$ -value of  $< 0.001$ , indicating that the correlations between variables are statistically significant and that the dataset is suitable for PCA. The results from the KMO measure and Bartlett's test of sphericity confirm the appropriateness of the dataset for PCA.

The PCA conducted on MRgFUS treatment data emphasized the paramount importance of individual anatomy in determining treatment effectiveness. After data normalization, the analysis revealed four principal components that together accounted for more than 84% of the variance in the dataset. The most significant variables for these components (Table 3),

based on the magnitude of their loadings, were:

- PC1 (Eigenvalue: 3.85): The most significant variable was the **maximum energy delivered (Joules)**, with a high coefficient of 0.45, indicating a strong influence of energy delivery on treatment outcomes.
- PC2 (Eigenvalue: 2.55): The **normalized CSFV** was identified as the key variable, with a coefficient of 0.55, underscoring the importance of CSFV in the treatment process.
- PC3 (Eigenvalue: 1.50): The **normalized WMV** was the most influential variable, with a coefficient of 0.60, reflecting the impact of WMV on the treatment's effectiveness.
- PC4 (Eigenvalue: 1.18): The **number of active elements** used during the sonication process was significant, with a coefficient of 0.53, highlighting its role in the procedural aspects of the treatment.

Fig. 3 provides a visual depiction of the significance of each principal component. The blue line represents the variance explained by each principal component, while the red line shows the cumulative variance explained, highlighting diminishing points after the fourth component. The "knee" of the plot indicates the optimal number of components to retain, corresponding to the point where the increase in explained variance plateaus, thus guiding the selection of the most informative components for subsequent analysis.

## 5 Discussion

The application of PCA in our study has greatly enhanced our understanding of the complexities associated with MRgFUS treatments. By uncovering the

Table 10 Mean of MRI parameters of patients.

Parameters of Brain Structural	Mean $\pm$ SD
Normalized GMV (cm <sup>3</sup> )	326.3 $\pm$ 35.3
Normalized WMV (cm <sup>3</sup> )	292.8 $\pm$ 41.3
Normalized CSF (cm <sup>3</sup> )	377.5 $\pm$ 49.6
Normalized Brain Volume (GM + WM) (cm <sup>3</sup> )	619.1 $\pm$ 48.4
Total Cortical Thickness	2.61 $\pm$ 0.2
Fazekas Scale	3.0 $\pm$ 0.7

Legend: GMV: Gray Matter Volume; WMV: White Matter Volume; CSF: Cerebrospinal Fluid; SD= Standard Deviation.

Table 20 Mean of MRgFUS parameters of patients.

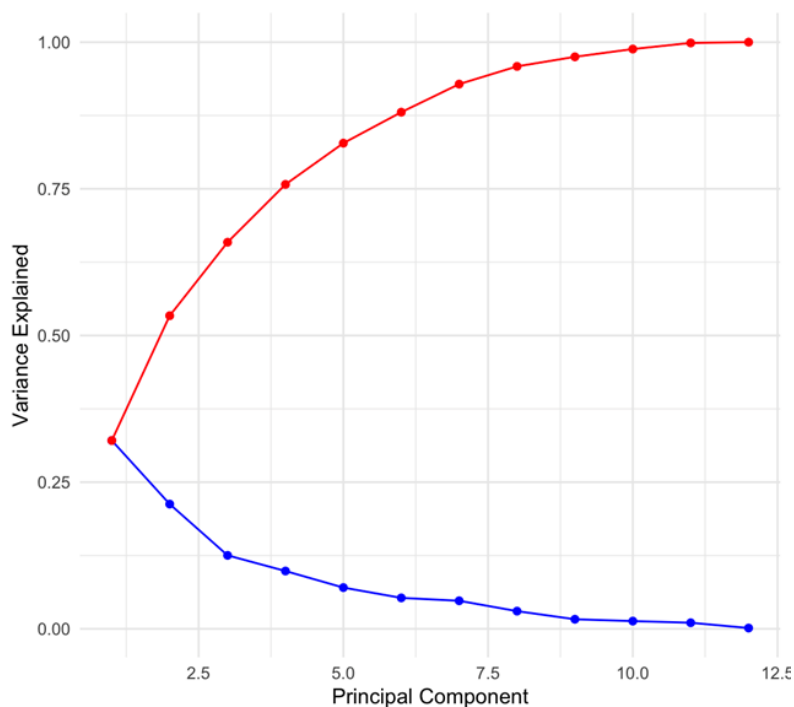
Parameters by MRgFUS	Mean $\pm$ SD
SDR	0.49 $\pm$ 0.12
Skull Area (cm)	338.6 $\pm$ 31.3
N° of Transducer Elements	906.6 $\pm$ 66.2
N° of Sonications	6.9 $\pm$ 2.1
maximal Watt	896.3 $\pm$ 139.5
maximal Joule	17673.6 $\pm$ 7413.7
maximal Temperature (T°C max)	57.4 $\pm$ 3.4
maximum Sonication Time (s)	22.9 $\pm$ 7.5
ATD	56.0 $\pm$ 2.9

Legend: SDR= Skull Density Ratio; ATD= Accumulated Thermal Dose; SD= Standard Deviation.

four principal components that together account for over 84% of the dataset variance, our analysis has reinforced the importance of high-dimensionality reduction in capturing essential characteristics of treatment data. Notably, the identification of maximum energy delivered, CSFV, WMV and active elements during sonication as the most significant variables mirrors findings from other studies which have emphasized the relevance of these variables in optimizing treatment efficacy and safety. Few studies have highlighted the influence of energy delivery on treatment outcomes, aligning with our results where maximum energy delivered (Joules) (PC1) demonstrated a predominant impact. [32], discussed the importance of precise energy delivery and the use of an autofocus echo imaging technique to enhance the safety and efficacy of MRgFUS treatments. This is crucial for patients with lower skull density ratios who might not otherwise benefit optimally from this technology. They explored these methods in a clinical trial setting, focusing on their impact on patients with essential tremor and Parkinson's disease. It details the techniques used and the outcomes observed, emphasizing the critical role of precise targeting and energy application. This approach is effective for treating neurological disorders, especially by overcoming challenges such as the skull's irregular structure, which can impede ultrasonic energy, [32]. These findings are in line with our results where maximum energy

delivered (PC1) shows a predominant impact on treatment outcomes. Infact, in our results, the coefficient of 0.45 for maximum energy delivered (Joule) in the first principal component signifies a strong influence of energy delivery on this component. This suggests that variations in the energy delivered during treatment are a dominant factor in explaining the variance captured by PC1. The larger the absolute value of the loading, the more significant the role of the variable in shaping the component. This implies that differences in treatment efficacy could be greatly impacted by how much energy is applied during the procedure. Furthermore, the variability in patient anatomy, such as skull density, also affects the energy delivery and subsequent treatment efficacy. Studies have found that patients with lower skull density ratios might experience different outcomes, emphasizing the need to adjust energy levels based on individual patient characteristics to optimize results. [33], examined the clinical outcomes of MRgFUS thalamotomy based on different SDRs, finding that while MRgFUS treatment can be effectively and safely performed in patients with lower SDRs, the procedure tends to be more efficient when the SDR is higher than 0.45. The study reported no significant differences in improvement in tremor severity among different SDR groups, although achieving the target temperature was more challenging in patients with lower SDRs. [34], analyzed the distribution of skull score (SS) and SDR





'Fig03: Cumulative Variance Explained for MRgFUS treatment data

Table 30 Summary of Principal Components Analysis Results

Principal Component	Most Significant Variable	Eigenvalues	Absolute Coefficients
PC1	maximum Energy Delivered (Joule)	3.85	0.45
PC2	Cerebrospinal Fluid Volume Normalized	2.55	0.55
PC3	White Matter Volume Normalized	1.50	0.60
PC4	Active Elements	1.18	0.53

in Taiwanese tremor patients, highlighting the challenges in achieving effective MRgFUS thalamotomy outcomes in patients with lower SS, as these often correlated with lower SDRs. This study suggests that half of the patients could have difficulties in reaching the therapeutic temperature necessary for successful treatment due to lower SDR. These findings support the significance of energy delivery in MRgFUS treatments, corroborating with the pivotal role highlighted by maximum energy delivered (PC1) in our study. This connection between the amount of energy delivered and the efficacy of treatment outcomes is well-established in the field, further underscoring the value of your PCA analysis in identifying key treatment variables. In addition, several studies emphasize the significance of these factors in the context of neurological diseases and treatments. For instance, the importance of CSFV is well recognized in managing brain physiology and its response to therapeutic interventions, [35], [36]. In our results, the coefficient of 0.55 indicates that CSFV significantly shapes

the second principal component. This highlights the importance of CSFV in the dataset, suggesting that variations in this parameter are key to understanding differences in the PCA model. It reflects how patient-specific anatomical features, like CSFV, can influence treatment outcomes. Similarly, WMV has been explored in the context of brain health and disease, pointing towards its relevance in understanding and treating neurological conditions, [35], [36]. In our results, we identified a coefficient of 0.60, highlighting that WMV is particularly influential in the third principal component. This finding emphasizes the importance of brain structure in treatment efficacy, suggesting that variations in WMV among patients are crucial to the differences observed in this component. Finally, active elements with a coefficient of 0.53 indicates a substantial contribution to the fourth principal component, emphasizing how aspects of the sonication process, such as the number of active elements used, play a significant role in the variance of the treatment data. This congruence un-

underscores the generalizability of our PCA approach in identifying key factors that affect treatment dynamics. Our study further delineates the relationships between anatomical and procedural variables, such as the linkage between CSFV and treatment efficacy noted in other works. CSFV is a crucial anatomical factor that influences how ultrasonic energy is propagated and absorbed during MRgFUS treatment. CSF, being a fluid present around the brain and spinal cord, can act as a medium that modulates the distribution of ultrasonic waves. Specifically, CSFV can attenuate or refract sound waves, affecting the ability to reach the therapeutic temperatures necessary for effective treatment. These relationships are critical for developing personalized treatment plans that are tailored to the individual anatomical and physiological characteristics of patients, also by interpretation with other neurophysiological approaches, [37].

## 6 Conclusion

Our PCA-based analysis integrates MRI parameters with MRgFUS treatment data, providing an approach that previous studies have not considered. [38], investigated MRgFUS in essential tremor patients and highlighted the importance of lesion size and location for predicting clinical outcomes. Similarly, in the study, [39], clinical outcomes were assessed in patients with symptomatic bone metastases using apparent diffusion coefficient (ADC) and dynamic contrast-enhanced (DCE) MRI, emphasizing the need for continuous monitoring of lesion dynamics post-treatment. [40], reviewed MRI follow-ups after MRgFUS thalamotomy, noting the significance of precise lesion targeting and its impact on clinical outcomes.

Unlike the above-mentioned papers, our study employs PCA to reduce data dimensionality and identify the most influential parameters, offering clearer insights into the key factors affecting patient prognosis. PCA enhances data interpretability and highlights the most significant parameters, providing a comprehensive treatment data to achieve a more predictive model for MRgFUS outcomes.

This integrated approach offers practical insights for clinicians, potentially improving patient selection and treatment planning, which is a step beyond the isolated parameter analysis. The application of PCA, as guided by Kaiser's rule, has not only facilitated a robust analysis of MRgFUS treatment variables but also set a benchmark for future research in the field. Its application in MRgFUS research, as demonstrated in [8], which examined learning curves and operator experience, can provide valuable insights for treatment optimization. The insights derived from our analysis offer a promising pathway for refining treatment protocols, enhancing the precision of MRgFUS therapies, and ultimately improving patient outcomes.

The visualization of data variance through the plot provided a clear and empirical basis for selecting the most informative components, an approach widely validated in contemporary studies that seek to simplify complex multidimensional data while retaining critical information. This study contributes to support the clinical value of PCA as a powerful analytical tool in the pursuit of personalized, precision-focused neurological treatment.

## References:

- [1] Ringnér M, What is principal component analysis?, *Nature Biotechnology*, Vol.26, No.3, 2008, pp. 303-304.
- [2] Margaritella N, Inácio V., King R., Parameter clustering in Bayesian functional principal component analysis of neuroscientific data, *Stat Med*, Vol.40, No.1, 2021, pp. 167-184.
- [3] Morabito R, Cammaroto S, Militi A, Smorto C, Anuso C, Lavano A, Tomasello F, Di Lorenzo G, Brigandì A, Sorbera C, Bonanno L, Ielo A, Vatrano M, Marino S, Cacciola A, Cerasa A, Quartarone A, The role of treatment-related parameters and brain morphology in the lesion volume of Magnetic-Resonance-Guided Focused Ultrasound thalamotomy in patients with tremor-dominant neurological conditions, *Bioengineering (Basel)*, Vol.11, No.4, 2024, pp. 373.
- [4] Begemann, Efficacy of non-invasive brain stimulation on cognitive functioning in brain disorders: a meta-analysis, *Psychological medicine*, Vol. 50, No. 15, 2020.
- [5] Benninger, Transcranial direct current stimulation for the treatment of Parkinson's disease, *Journal of Neurology, Neurosurgery & Psychiatry*, Vol. 81, No. 10, 2010.
- [6] Zhong, Low intensity focused ultrasound: a new prospect for the treatment of Parkinson's disease, *Annals of Medicine*, Vol. 55, No. 2, 2023.
- [7] Elias et al., A pilot study of focused ultrasound thalamotomy for essential tremor, *New England Journal of Medicine*, Vol. 369, No. 7, 2013.
- [8] Bruno F, Tommasino E, Pertici L, Pagliei V, Gagliardi A, Catalucci A, Arrigoni F, Palumbo P, Sucapane P, Pistoia F, Marini C, Ricci A, Barile A, Di Cesare E, Splendiani A, Masciocchi C. MRgFUS thalamotomy for the treatment of tremor: evaluation of learning curve and operator's experience impact on the procedural and clinical outcome, *Acta Neurochir (Wien)*, Vol.165, No.3, 2023, pp. 727-733.

- [9] Elias WJ, Lipsman N, Ondo WG, et al, A randomized trial of focused ultrasound thalamotomy for essential tremor, *N Engl J Med* Vol.375, 2016, pp. 730–739.
- [10] McDannold NJ, King RL, Jolesz FA, Hynynen KH. Usefulness of MR imaging-derived thermometry and dosimetry in determining the threshold for tissue damage induced by thermal surgery in rabbits, *Radiology*, Vol.216, No.2, 2000, pp.517-23.
- [11] Schuurman PR, Bosch DA, Merkus MP, Speelman JD. Long-term follow-up of thalamic stimulation versus thalamotomy for tremor suppression, *Mov Disord*, Vol.23, No.8, 2008, pp.1146-53.
- [12] Lipsman N, Schwartz ML, Huang Y, et al. MR-guided focused ultrasound thalamotomy for essential tremor: a proof-of-concept study, *Lancet Neurol*, Vol.12, 2013, pp. 462–468.
- [13] Chang WS, Jung HH, Zadicario E, et al. Factors associated with successful magnetic resonance-guided focused ultrasound treatment: efficiency of acoustic energy delivery through the skull, *J Neurosurg*, Vol. 124, 2016, pp. 411–416.
- [14] Gagliardo C, Cannella R, Filorizzo G, Toia P, Salvaggio G, Collura G, Pignolo A, Maugeri R, Napoli A, D’amelio M, Bartolotta TV, Marrale M, Iacopino GD, Catalano C, Midiri M. Preoperative imaging findings in patients undergoing transcranial magnetic resonance imaging-guided focused ultrasound thalamotomy, *Sci Rep* Vol.11, No. 1, 2021, pp. 2524
- [15] Otsu, N, A threshold selection method from gray-level histograms, *IEEE Trans. Syst. Man Cybernetics* Vol.9, 1979, pp. 62–66.
- [16] Chang K. W., Park Y.S., Chang J.W., Skull factors affecting outcomes of magnetic resonance-guided focused ultrasound for patients with essential tremor, *Yonsei Med J*, Vol. 60, 2019, pp. 768–773.
- [17] D’Souza M, Chen KS, Rosenberg J, Elias WJ, Eisenberg HM, Gwinn R, Taira T, Chang JW, Lipsman N, Krishna V, Igase K, Yamada K, Kishima H, Cosgrove R, Rumià J, Kaplitt MG, Hirabayashi H, Nandi D, Henderson JM, Butts Pauly K, Dayan M, Halpern CH, Ghanouni P, Impact of skull density ratio on efficacy and safety of magnetic resonance-guided focused ultrasound treatment of essential tremor, *J Neurosurg* Vol. 132, No.5, 2019, pp. 1392-1397.
- [18] Sinai A, Nassar M, Eran A, Constantinescu M, Zaaroor M, Sprecher E, Schlesinger I. Magnetic resonance-guided focused ultrasound thalamotomy for essential tremor: a 5-year single-center experience, *J Neurosurg*, Vol.5, 2019, pp. 1-8.
- [19] Yamamoto K, Ito H, Fukutake S, Odo T, Kamei T, Yamaguchi T, et al. Factors Associated with Heating Efficiency in Transcranial Focused Ultrasound Therapy, *Neurol Med Chir (Tokyo)*, 2020.
- [20] Huang Y, Lipsman N, Schwartz ML, Krishna V, Sammartino F, Lozano AM, Hynynen K. Predicting lesion size by accumulated thermal dose in MR-guided focused ultrasound for essential tremor, *Med Phys*, Vol. 45, No. 10, 2018, pp.4704-4710.
- [21] Bond AE, Elias WJ. Predicting lesion size during focused ultrasound thalamotomy: a review of 63 lesions over 3 clinical trials, *Neurosurg Focus* Vol. 44, 2018, pp. E5.
- [22] Post M, Wolf S, Stock G, Principal component analysis of nonequilibrium molecular dynamics simulations, *J Chem Phys* ., Vol.150, No.20, 2019, pp. 204110.
- [23] Sawyer C, Green J, Lim B, Pobric G, Jung JY, Vassallo G, Evans DG, Stagg CJ, Parkes LM, Stivaros S, Muhlert N, Garg S, Neuroanatomical correlates of working memory performance in Neurofibromatosis 1, *Cereb Cortex Commun*, Vol.3, No.2, 2022, pp. 1-9.
- [24] Defer GL, Widner H, Marié RM, Rémy P, Levivier M. Core assessment program for surgical interventional therapies in Parkinson’s disease (CAPSIT-PD), *Mov Disord*, Vol.14, No.4, 1999, pp. 572-584.
- [25] Colucci V, Strichartz G, Jolesz F, Vykhodtseva N, Hynynen K, Focused ultrasound effects on nerve action potential in vitro, *Ultrasound in medicine & biology*, Vol.35, No.10, 2009, pp. 1737-1747.
- [26] Foley JL, Little JW, Vaezy S, Image-guided high-intensity focused ultrasound for conduction block of peripheral nerves, *Annals of biomedical engineering* Vol.35, No.1, 2007, pp. 109-119.
- [27] van Vliet EA, da Costa Araujo S, Redeker S, van Schaik R, Aronica E, Gorter JA, Blood-brain barrier leakage may lead to progression of temporal lobe epilepsy, *Brain*, Vo. 130, 2007, pp. 521–523.

- [28] Cole JH, Jolly A, De Simoni S, et al. Spatial patterns of progressive brain volume loss after moderate-severe traumatic brain injury, *Brain* Vol.141, No.3, 2018, pp. 822–836
- [29] Dahnke R, Yotter RA, Gaser C. Cortical thickness and central surface estimation, *Neuroimage* Vol.65, 2013, pp. 336–348.
- [30] Yotter RA, Dahnke R, Thompson PM, et al. Topological correction of brain surface meshes using spherical harmonics, *Hum Brain Mapp* Vol.32, 2011, pp. 1109–1124
- [31] Fazekas F, Chawluk JB, Alavi A, Hurtig HI, Zimmerman RA. MR signal abnormalities at 1.5 T in Alzheimer's dementia and normal aging, *AJR Am J Roentgenol*, Vol.149, No.2, 1987, pp. 351–356.
- [32] Chang KW, Rachmilevitch I, Chang WS, Jung HH, Zadicario E, Prus O, Chang JW. Safety and Efficacy of Magnetic Resonance-Guided Focused Ultrasound Surgery With Autofocusing Echo Imaging, *Front Neurosci.*, Vol.12, 2021, pp.592763
- [33] D'Souza M, Chen KS, Rosenberg J, Elias WJ, Eisenberg HM, Gwinn R, Taira T, Chang JW, Lipsman N, Krishna V, Igase K, Yamada K, Kishima H, Cosgrove R, Rumià J, Kaplitt MG, Hirabayashi H, Nandi D, Henderson JM, Butts Pauly K, Dayan M, Halpern CH, Ghanouni P, Impact of skull density ratio on efficacy and safety of magnetic resonance-guided focused ultrasound treatment of essential tremor, *J Neurosurg*, Vol.132, No.5, 2019, pp. 1392–1397.
- [34] Tsai KW, Chen JC, Lai HC, Chang WC, Taira T, Chang JW, Wei CY. The Distribution of Skull Score and Skull Density Ratio in Tremor Patients for MR-Guided Focused Ultrasound Thalamotomy, *Front Neurosci*, Vol.15, 2021, pp.612940.
- [35] Doron O, Zadka Y, Barnea O et al., Interactions of brain, blood, and CSF: a novel mathematical model of cerebral edema, *Fluids and Barriers of the CNS*, Vol.18, No.42, 2021.
- [36] Liu G., Ladrón-de-Guevara A, Izhiman Y. et al., Measurements of cerebrospinal fluid production: a review of the limitations and advantages of current methodologies, *Fluids Barriers CNS*, Vol.19, No.101, 2022.
- [37] Gurgone S, De Salvo S, Bonanno L, Muscarà N, Acri G, Caridi F, Paladini G, Borzelli D, Brigandi A, La Torre D, Sorbera C, Anfuso C, Di Lorenzo G, Venuti V, d'Avella A, Marino S, Changes in cerebral cortex activity during a simple motor task after MRgFUS treatment in patients affected by essential tremor and Parkinson's disease: a pilot study using functional NIRS, *Phys Med Biol.*, Vol.11, No.2, 2024.
- [38] Kapadia et al., Multimodal MRI for MRgFUS in essential tremor: post-treatment radiological markers of clinical outcome *Journal of Neurology, Neurosurgery & Psychiatry*, Vol. 91, No.9, 2020.
- [39] Anzidei et al., Magnetic resonance-guided focused ultrasound for the treatment of painful bone metastases: role of apparent diffusion coefficient (ADC) and dynamic contrast enhanced (DCE) MRI in the assessment of clinical outcome, *La radiologia medica*, Vol. 121, pp. 905–915, 2016.
- [40] Keil et al., MRI follow-up after magnetic resonance-guided focused ultrasound for non-invasive thalamotomy: the neuroradiologist's perspective, *Neuroradiology*, Vol. 62, 2020.

#### Contribution of Individual Authors to the Creation of a Scientific Article (Ghostwriting Policy)

Lilla Bonanno has formulated the research goals and aims, developed the methodology, performed the data analysis and written the original draft. Augusto Ielo, Serena Dattola and Valentina Hartwig have collaborated to the data presentation. Rosa Morabito, Simona Cammaroto, Chiara Smorto, Annalisa Militi, Carmelo Anfuso have organized and executed the MRgFUS exams. Giuseppe Di Lorenzo, Chiara Sorbera, Amelia Brigandi and Silvia Marino have collected the data. Alberto Cacciola and Antonio Cerasa have supervised the research activity. Angelo Quartarone has acquired the funding. Giuseppe Acri has reviewed the original draft and supervised the research activity.

#### Sources of Funding for Research Presented in a Scientific Article or Scientific Article Itself

**This work was supported by DOD N° W81XWH-19-1-0810 (AQ). This study was also funded by the 2023 research funds of the Italian Ministry of Health.**

### **Conflict of Interest**

The authors have no conflicts of interest to declare.

### **Creative Commons Attribution License 4.0 (Attribution 4.0 International, CC BY 4.0)**

This article is published under the terms of the Creative Commons Attribution License 4.0

[https://creativecommons.org/licenses/by/4.0/deed.en\\_US](https://creativecommons.org/licenses/by/4.0/deed.en_US)